Band structure and shape coexistence in $^{135}_{56}Ba_{79}$

Suresh Kumar,[1,2,*] A. K. Jain,[1] Alpana Goel,[3] S. S. Malik,[4] R. Palit,[5] H. C. Jain,[5] I. Mazumdar,[5] P. K. Joshi,[5] Z. Naik,[5] A. Dhal,[6] T. Trivedi,[7] I. Mehrotra,[7] S. Appannababu,[8] L. Chaturvedi,[9] V. Kumar,[10] R. Kumar,[10] D. Negi,[10] R. P. Singh,[10] S. Muralithar,[10] R. K. Bhowmik,[10] and S. C. Pancholi[2,10]

[1]*Department of Physics, Indian Institute of Technology, Roorkee 247667, India*
[2]*Department of Physics and Astrophysics, University of Delhi, Delhi 110007, India*
[3]*Department of Physics, Amity University, Noida 201303, India*
[4]*Department of Physics, Guru Nanak Dev University, Amritsar 143005, India*
[5]*Department of Nuclear and Atomic Physics, Tata Institute of Fundamental Research, Mumbai 400005, India*
[6]*Department of Physics, Banaras Hindu University, Varanasi 221005, India*
[7]*Department of Physics, University of Allahabad, Allahabad 211002, India*
[8]*Department of Nuclear Physics, The Maharaja Sayajirao University, Borada 390002, India*
[9]*Guru Ghasidas University, Bilaspur, Chhattisgarh 495009, India*
[10]*Inter University Accelerator Centre, Aruna Asaf Ali Marg, New Delhi 110067, India*

(Received 14 October 2009; revised manuscript received 10 May 2010; published 22 June 2010)

Excited states of $^{135}_{56}Ba_{79}$ at high spins are studied using the reaction ^{130}Te(^{9}Be,4n)$^{135}_{56}Ba_{79}$ at 42.5-MeV beam energy. The earlier known level scheme is extended up to 6.4-MeV excitation energy and $(37/2)\hbar$ spin with the addition of several transitions. We have performed polarization asymmetry measurements for some of the strong transitions by using a Clover detector to assign the parity. A comparison of experimental data with the results of tilted axis cranking calculations based on various configurations indicates the coexistence of multiple minima in the triaxial deformation (γ), whereas axial symmetric deformation (ϵ_2) remains constant around 0.09.

DOI: 10.1103/PhysRevC.81.067304 PACS number(s): 21.10.Hw, 21.60.Cs, 23.20.−g, 27.60.+j

Nuclei in the $A \approx 135$ mass region are transitional in nature with moderate deformation and soft with respect to the triaxialty parameter (γ). Nilsson diagrams indicate that in this mass region there are several positive-parity orbitals originating from the $g_{7/2}$, $d_{5/2}$, $d_{3/2}$, and $s_{1/2}$ spherical shell-model states which determine the low-energy structure, whereas for the negative-parity states there is only the $h_{11/2}$ orbital. Many of these nuclei show interesting spectroscopic properties both at low and high spins [1–4]. In the odd-mass even-Z nuclei ($N \leqslant 77$), collective structures based on the $h_{11/2}$ and $g_{7/2}$ neutron configurations have been systematically observed and characterized as having a triaxial prolate shape [5,6]. Recently, ^{139}Nd [2,7] and ^{137}Ce [8] nuclei have been studied to high spins. Both these nuclei have shown bands based on multiquasiparticle configuration and shape coexistence phenomenon. In earlier works, some low-spin states in $^{135}_{56}Ba_{79}$ were observed in Coulomb excitation [9], in the β-decay mode [10,11], in the (n,γ) reaction [11], and in the (^{9}Be,4n) reaction [12,13]. In the present work, we have studied the multiquasiparticle bands at high spins. Spins and parities of the levels have been assigned from a directional correlation of oriented nuclei (DCO) ratios and linear polarization of the γ-ray, respectively. The observation of new crossover $E2$ transitions in two of the bands required some modification in the earlier reported work [13]. The experimental results have been compared with a hybrid version of the tilted axis cranking (TAC) model [14] calculations.

The high-spin states of $^{135}_{56}Ba_{79}$ were populated using the ^{130}Te(^{9}Be,4n)$^{135}_{56}Ba_{79}$ reaction. The 42.5-MeV ^{9}Be beam was delivered by the 15-UD Pelletron Accelerator at Inter University Accelerator Centre (IUAC), New Delhi. The target consisted of 750 μg/cm^2 of enriched ^{130}Te deposited on a 6 mg/cm^2 gold backing. The γ-γ coincidence data were collected by using the Gamma Detector Array (GDA) [15]. For the measurement of linear polarization of γ-rays, a Clover detector [16] was set at a position of 98° in place of a HPGe detector, at a distance of 22 cm from the target. A total of 240×10^6 γ-γ events (twofold and higher) were sorted out into an E_γ-E_γ (4k × 4k) matrix using the CANDLE program (an acquisition system developed at IUAC, New Delhi) and analyzed by using the RADWARE package [17].

The level scheme obtained from the present work is shown in Fig. 1. A total of 20 new γ-rays have been found and placed in the level scheme. The γ-ray energies, their relative intensities, $R_{\rm DCO}$, and linear polarization asymmetries are listed in Table I. The sequence of negative-parity yrast states, which was built on the $11/2^-$ isomer, was known from Refs. [12,13] up to the $19/2^-$ state at 2002.6 keV. In [13], it was suggested that the low-spin states in $^{135}_{56}Ba_{79}$ have a triaxial shape with $\gamma > 30°$. In the present work, we have confirmed the spin and parity of the 950.5- and 2002.6-keV states by using the value of polarization asymmetry and $R_{\rm DCO}$ values. In addition, we have observed a new state at 2089.4 keV ($19/2^-$), which decays to the 950.5-keV state $15/2^-$ by the 1138.9-keV γ-ray. This new state in turn is populated from the 2388.5-keV state (23/2) by a 299.1-keV γ-ray. The 2388.5-keV state also decays to the 2002.6-keV $19/2^-$ state by a 386.0-keV γ-ray. The $R_{\rm DCO}$ of the 254.4-keV and the $R_{\rm DCO}$ and polarization asymmetry value of the 1183.6-keV transition indicate that the former is a quadrupole transition and the latter is an $E2$ transition. The ground band appears to have a structure

*ranasvs@rediffmail.com

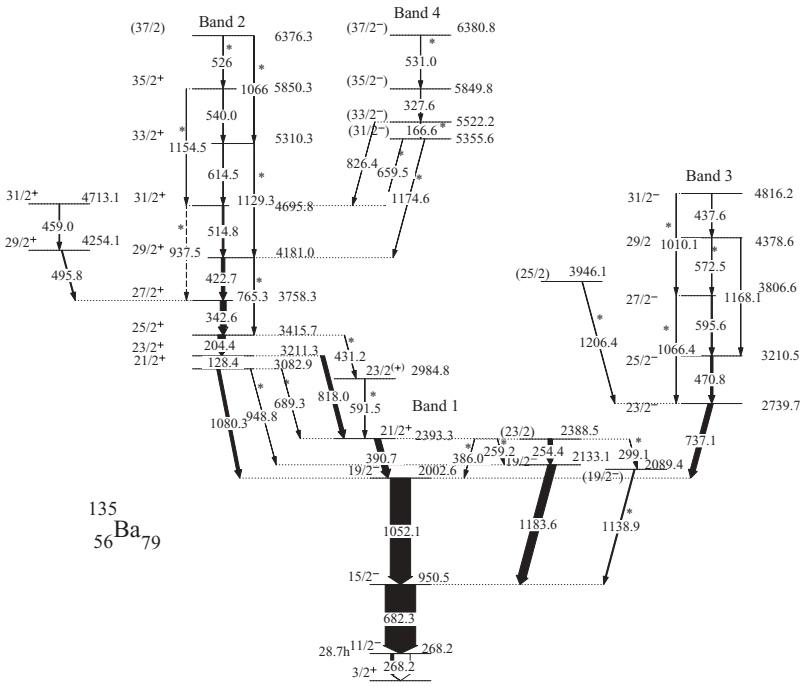

FIG. 1. Level scheme of $^{135}_{56}Ba_{79}$. The newly observed transitions from the present work are marked by stars.

similar to the other $N = 79$ even-Z nuclei [2,3,18,19]. The $21/2^+$ state at 2393.3-keV, which decays by the 390.7-keV $E1$ transition, may originate from the coupling of an $h_{11/2}$ neutron hole to the 5^- state $\nu(h_{11/2}^{-1}, s_{1/2}^{-1})$ of the core nucleus ^{136}Ba. Therefore, the $21/2^+$ state at 2393.3 keV may have a $\nu(h_{11/2}^{-2}, s_{1/2}^{-1})$ configuration with a minima obtained by the Nilsson-Strutinsky approach (using TAC calculations) at the deformation parameters $\epsilon_2 = 0.086$ and $\gamma = -15^\circ$ (with a tilt angle $\approx 78.2^\circ$).

Band 2 is based on the band head $I = 21/2^+$ level at 3082.9 keV. The decay out of the levels at 3082.9 and 3211.3 keV proceeds through several transitions to the 2002.6-keV state of the ground band (see Fig. 1). The R_{DCO} and polarization asymmetry of the strong transitions 390.7, 818.0, and 1080.3 keV are used to assign the spin of the band head (see Table I). The sum-gate spectrum gated on $128.4 + 204.4 + 342.6$ keV [Fig. 2(a)] contains the low-lying transitions fed through the depopulation of the $\Delta I = 1$ band and the γ-rays belonging to the members of the $\Delta I = 1$ band. The band contains 128.4-, 204.4-, 342.6-, 422.7-, 514.8-, 614.5-, 540.0-, and 526.0-keV $\Delta I = 1$ transitions [Fig. 2(a)] and 765.3-, 937.5-, 1129.3-, 1154.5-, and 1066.0-keV crossover $\Delta I = 2$ transitions [Fig. 2(b)]. As is evident from Fig. 2(b), one of the crossover transitions between $31/2^+$ to $27/2^+$ with energy 937.5 keV was found to be quite weak compared to other $E2$ transitions in this band. The placement of 514.8- and 614.5-keV transitions has been reversed in contrast to earlier work [13] on the basis of the coincidence and anticoincidence relationship of $E2$ crossover transitions. The 1154.5-keV crossover transition is present in the gate of 514.8 keV [Fig. 2(c)], but not in the gate of 614.5 keV [Fig. 2(d)], which shows that the 1154.5-keV transition is above the 4695.8-keV level. The experimental $B(M1)/B(E2)$ ratios for band 2 are shown in Fig. 3(b) and show a staggering behavior which is similar to the behavior of the $B(M1)/B(E2)$ ratios seen in the band based on the configuration $\pi(h_{11/2}g_{7/2}) \otimes \nu(h_{11/2})^{-1}$ in $N = 77$ even-Z nuclei (band 2 in ^{133}Ba [20] and band 5 in ^{137}Nd [1]). A three quasiparticle (qp) $\pi(h_{11/2}g_{7/2}) \otimes \nu(h_{11/2})^{-1}$ was, therefore, used in the TAC calculations for the positive-parity dipole band. The pairing parameters Δ_p and Δ_n, calculated as 80% of the odd-even mass difference, are 0.896 and 0.926 MeV, respectively. A minimum was found at the deformation parameters $\epsilon_2 = 0.095, \epsilon_4 = -0.013, \gamma = 26^\circ$ with an average tilt angle $\approx 56.4^\circ$ which corresponds to a triaxial shape. The calculations based on this configuration seem to explain the observed behavior of E versus $I(\hbar)$ as shown in Fig. 4. The calculated results reasonably agree with the measured values. The experimental $I(\hbar)$ versus $\hbar\omega$ plot, as shown in Fig. 3(a), is also nicely explained by the calculations. The calculated $B(M1)/B(E2)$ values for deformation parameters $\epsilon_2 = 0.095, \epsilon_4 = -0.013, \gamma = 26^\circ$ are large compared to the experimental values, whereas the calculation for deformation parameters $\epsilon_2 = 0.095, \epsilon_4 = -0.013, \gamma = 10^\circ$ (not a self-consistent minima) explain the experimental $B(M1)/B(E2)$ ratios [see Fig. 3(b)]. The calculated $B(M1)$ values decrease with an increase in $\hbar\omega$ (i.e., from 2.9 to 1.2 μ_N^2) while $B(E2)$ values increase with an increase in $\hbar\omega$ [i.e., from 0.010 to 0.025 $(eb)^2$] (not shown in Fig. 3). Thus, based on the systematics and the TAC calculations, we suggest that the positive-parity dipole band 2 built on the 3082.8-keV state has the $\pi(h_{11/2}g_{7/2}) \otimes \nu h_{11/2}^{-1}$ 3qp configuration, and may have a magnetic rotation behavior.

Band 3, established in the present work, is based on the 2739.7-keV $23/2^-$ level (see Fig. 1). The band head directly feeds the 2002.6-keV $19/2^-$ level by the 737.1-keV $E2$ transition, confirming the $23/2^-$ assignment for it. The intraband 470.8-, 595.6-, 572.5-, and 437.6-keV transitions have been observed along with the crossover 1066.4-, 1168.1-, and 1010.1-keV transitions as shown in the sum gates of Fig. 2(f). We have also observed a single 1206.4-keV transition feeding into the 2739.7-keV $23/2^-$ level

TABLE I. Gamma ray energy (E_γ), relative intensity (I_γ), $R_{\rm DCO}$, polarization asymmetry (Δ) ratios, assigned multipolarity (MP), and spin for γ transitions in $^{135}_{56}Ba_{79}$. Superscript Q's indicate gated on a 682.3 quadrupole transition and superscript D's indicate gated on a 204.4 dipole transition.

E_γ (keV)	I_γ	$R_{\rm DCO}$	Δ ratios	MP	J_i^π	J_f^π
128.4	7.6(12)	0.64(11)^Q		D	$23/2^+$	$21/2^+$
166.6	1.59(18)	0.68(19)^Q		D	$(33/2^-)$	$(31/2^-)$
204.4	21.8(8)	0.65(5)^Q	−0.08(2)	$M1$	$25/2^+$	$23/2^+$
254.4	12.9(11)	1.13(12)^Q		Q	(23/2)	$19/2^-$
259.2	0.57(16)				$21/2^+$	$19/2^-$
268.2				$M4$[a]	$11/2^-$	$3/2^+$
299.1	1.07(23)				(23/2)	(19/2)
327.6	1.38(19)	0.62(18)^Q		D	$(35/2^-)$	$(33/2^-)$
342.6	18.2(11)	0.67(7)^Q	−0.05(3)	$M1$	$27/2^+$	$25/2^+$
386.0	1.03(21)				(23/2)	$19/2^-$
390.7	19.9(9)	0.61(6)^Q	0.07(2)	$E1$	$21/2^+$	$19/2^-$
422.7	11.3(12)	0.46(8)^Q	−0.02(2)	$M1$	$29/2^+$	$27/2^+$
431.2	1.66(23)				$25/2^+$	$23/2^{(+)}$
437.6	1.05(20)				$31/2^-$	$29/2^-$
459.0	2.4(12)	0.46(18)^Q		D	$31/2^+$	$29/2^+$
470.8	7.9(8)	0.61(12)^Q	−0.13(6)	$M1$	$25/2^-$	$23/2^-$
495.8	3.36(21)	0.64(11)^Q		D	$29/2^+$	$27/2^+$
514.8	5.60(23)	0.56(13)^Q		D	$31/2^+$	$29/2^+$
526.0	1.05(24)				$(37/2^+)$	$35/2^+$
531.0	1.17(16)	0.39(17)^Q		D	$(37/2^-)$	$(35/2^-)$
540.0	1.63(17)	0.46(20)^Q		D	$35/2^+$	$33/2^+$
572.5	0.54(15)			D	$29/2^-$	$27/2^-$
591.5	1.71(12)				$23/2^{(+)}$	$21/2^+$
595.6	4.1(11)			D	$27/2^-$	$25/2^-$
614.5	2.1(12)	0.80(21)^D		D	$33/2^+$	$31/2^+$
659.5	0.60(21)				$(31/2^-)$	$31/2^+$
682.3	100.0	1.47(10)^D	0.10(3)	$E2$	$15/2^-$	$11/2^-$
689.3	0.74(12)				$21/2^+$	$21/2^+$
737.1	16.8(8)	0.86(15)^Q	0.24(9)	$E2$	$23/2^-$	$19/2^-$
765.3	1.58(16)	1.49(25)^D		$(E2)$	$29/2^+$	$25/2^+$
818.0	13.1(7)	0.69(8)^Q	−0.03(2)	$M1$	$23/2^+$	$21/2^+$
826.4	0.9(16)				$(33/2^-)$	$31/2^+$
937.5	0.40(18)			$(E2)$	$31/2^+$	$27/2^+$
948.8	0.78(13)				$21/2^+$	$19/2^-$
1010.1	0.86(16)			$(E2)$	$31/2^-$	$27/2^-$
1052.1	67.5(3)	0.99(6)^Q	0.09(3)	$E2$	$19/2^-$	$15/2^-$
1066.4	1.50(23)			$(E2)$	$27/2^-$	$23/2^-$
1080.6	10.4(12)	0.66(11)^Q	0.06(4)	$E1$	$21/2^+$	$19/2^-$
1129.3	1.04(23)			$(E2)$	$33/2^+$	$29/2^+$
1138.9	3.8(10)				(19/2)	$15/2^-$
1154.9	0.68(18)			$(E2)$	$35/2^+$	$31/2^+$
1168.1	1.5(13)			$(E2)$	$29/2^-$	$25/2^-$
1174.6	1.4(15)				$(31/2^-)$	$29/2^+$
1183.6	26.9(8)	0.80(10)^Q	0.13(5)	$E2$	$19/2^-$	$15/2^-$
1206.4	1.9(3)				(25/2)	$21/2^-$

[a]Taken from Ref. [11].

of the band. A structure in ^{133}Ba, referred to as band 7 in Ref. [20], is similar to band 3 in $^{135}_{56}Ba_{79}$ (Fig. 1) and was proposed to have the $\pi(g_{7/2}d_{5/2}) \otimes \nu h_{11/2}^{-1}$ configuration. Due to the similarity in the band structure and the behavior of $B(M1)/B(E2)$ of both the isotopes, it is possible that band 3 may possess a similar configuration. Thus, we have adopted

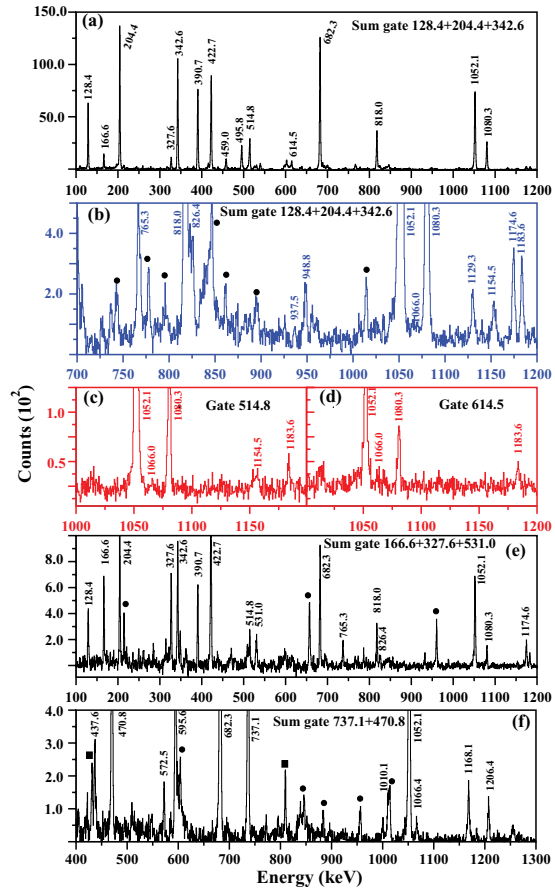

FIG. 2. (Color online) The spectra obtained by a sum gate and a gate on various transitions showing the γ-rays associated with $^{135}_{56}Ba_{79}$. The peaks marked with circles are contaminants and the peaks marked with squares may belong to $^{135}_{56}Ba_{79}$, but they are not placed in a level scheme.

the $\pi[g_{7/2}(g_{7/2}/d_{5/2})^1] \otimes \nu h_{11/2}^{-1}$ configuration for band 3. The TAC calculations have been carried out for two situations: one corresponding to the $(g_{7/2}/d_{5/2})$ proton placed in the second orbital and the other corresponding to the $(g_{7/2}/d_{5/2})$ proton placed in the third orbital from the Fermi level of the TAC quasiproton Routhian. We obtain minima at $\epsilon_2 = 0.085$, $\epsilon_4 = 0.0$, $\gamma = -15^\circ$ and $\epsilon_2 = 0.090$, $\epsilon_4 = 0.0$, $\gamma = -10^\circ$ for the two situations, respectively. We have plotted the experimental data and the results of the TAC calculations in Figs. 3(c) and 3(d)). The I versus $\hbar\omega$ plots do not match very well but the E versus $I(\hbar)$ plot (see Fig. 4) does explain the experimental data very well. The calculated $B(M1)/B(E2)$ ratios are of the same order as the measured $B(M1)/B(E2)$ ratios. The $B(M1)$ values (ranging from 0.60 to 0.10 μ_N^2) as well as the $B(M1)/B(E2)$ ratios are not large and they do not satisfy the criteria of magnetic rotation.

Band 4 has been observed to feed the 4181.0- and 4695.8-keV levels of band 2 by the 1174.6- and 826.4-keV transitions. The sum-gated spectrum is shown in Fig. 2(e). The $\Delta I = 1$ sequence that consists of 166.6, 327.6, and 531.0 γ-rays has a similar structure and band-head energy as seen in band 4 of ^{137}Ce [3] or band 6 of ^{137}Ce [8], band 1 of ^{139}Nd [7], and band 4 of ^{133}Ba [20]. The tentative spin and

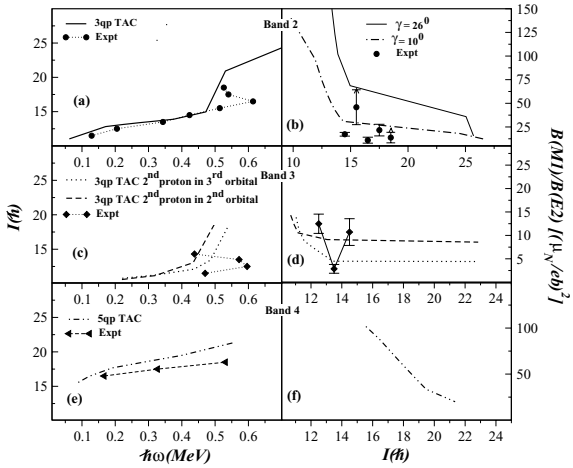

FIG. 3. A comparison of the experimental results with the results of TAC calculations for bands 2, 3, and 4.

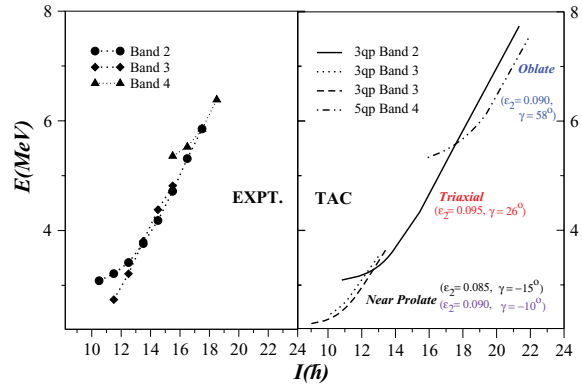

FIG. 4. (Color online) Plot showing the E vs $I(\hbar)$ behavior for the measured (right panel) and the calculated (left panel) values of bands 2, 3 and 4.

parity assignments of this band are based on a comparison with the collective band in ^{137}Ce. A similar band structure has also been observed in $N \leqslant 77$ even-Z nuclei [1,6]. TAC calculations have been performed for this band by using the 5qp configuration $\pi(h_{11/2}g_{7/2}) \otimes \nu(h_{11/2})^2 s_{1/2}$. This leads us to a minimum at $\epsilon_2 = 0.090$, $\gamma = 58°$. The TAC results for $I(\hbar)$ and $B(M1)/B(E2)$ values for this configuration are plotted as a function of $\hbar\omega$ and $I(\hbar)$, respectively, in Figs. 3(e) and 3(f). The $B(M1)$ values (4.0 to 0.25 μ_N^2) as well as the $B(M1)/B(E2)$ ratios are seen to fall with the increasing $\hbar\omega$ for an average tilt angle of 34°. It may be noted that the calculated $B(M1)/B(E2)$ ratios are of the same order as the experimentally observed values in ^{133}Ba (band 4 in Ref. [20]). Thus, we propose that band 4 may be an oblate magnetic rotation band with a 5qp $\pi(h_{11/2}g_{7/2}) \otimes \nu(h_{11/2})^2 s_{1/2}$ configuration.

Finally, an overall view of the measured and calculated (TAC results) E versus $I(\hbar)$ behavior for all bands, excluding the ground band, can be seen in Fig. 4, respectively. Band 3 is the first one to become yrast by crossing the ground band (not shown in the left panel of Fig. 4). Band 2 then crosses band 3 to become yrast followed by band 4 which crosses band 2. The results of the TAC calculations for bands 2, 3, and 4 for the parameter values discussed earlier are plotted in the right panel of Fig. 4. It may be observed that the excitation energy pattern as well as the crossings are reproduced reasonably well in all cases.

In summary, besides confirmation and modification of the previous level scheme, identification was made of approximately 20 new γ transitions that comprise three band structures at high spins. The most striking result of the present work is the coexistence of a band structure that results from the existence of multiple minima in the γ deformation with $\epsilon_2 \approx 0.09$. The near prolate and triaxial bands have been observed to be based on the 3qp configurations (bands 2 and 3), while the oblate band has a 5qp configuration (band 4). Bands 2 and 4 also appear to be magnetically rotational by nature. Thus, the $^{135}_{56}Ba_{79}$ nucleus is a γ-soft nucleus and exhibits a shape coexistence of near prolate, triaxial, and oblate shapes at high spins. However, the $13/2^-$ state seen in other $N = 79$ even-Z nuclei could not be observed. For a better understanding of band 2, it is necessary to undertake additional experiments on lifetime measurements.

Financial support from the Ministry of Human Resources and Development and the Department of Science and Technology (Government of India) at Roorkee is gratefully acknowledged.

[1] C. M. Petrache *et al.*, Nucl. Phys. A **617**, 228 (1997).
[2] S. Kumar *et al.*, Phys. Rev. C **76**, 014306 (2007).
[3] S. J. Zhu *et al.*, Phys. Rev. C **62**, 044310 (2000).
[4] C. Rossi Alvarez *et al.*, Phys. Rev. C **54**, 57 (1996).
[5] A. Granderath, P. F. Mantica, R. Bengtsson, R. Wyss, P. Von Brentano, A. Gelberg, and F. Seiffert, Nucl. Phys. A **597**, 427 (1996).
[6] E. S. Paul, D. B. Fossan, Y. Liang, R. Ma, and N. Xu, Phys. Rev. C **40**, 1255 (1989).
[7] Q. Xu *et al.*, Phys. Rev. C **78**, 034310 (2008).
[8] T. Bhattacharjee *et al.*, Phys. Rev. C **78**, 024304 (2008).
[9] E. Dragulescu, M. Ivascu, R. Mihu, D. Popescu, G. Semenescu, A. Velenik, and V. Paar, J. Phys. G: Nucl. Phys. **10**, 1099 (1984).
[10] M. S. Fetea *et al.*, Phys. Rev. C **73**, 051301(R) (2006).
[11] B. Singh, A. A. Rodionov, and Y. L. Khazov, Nucl. Data Sheets **109**, 517 (2008).
[12] E. Dragulescu, M. Ivascu, G. Semenescu, I. Gurgu, L. Marinescu, and I. Baciu, Rev. Roum. Phys. **32**, 743 (1987).
[13] X. L. Che *et al.*, Eur. Phys. J. A **30**, 347 (2006).
[14] V. I. Dimitrov, F. Dönau, and S. Frauendorf, Phys. Rev. C **62**, 024315 (2000).
[15] S. C. Pancholi and R. K. Bhowmik, Ind. J. Pure & Appl. Phys. **27**, 660 (1989).
[16] R. Palit, H. C. Jain, P. K. Joshi, S. Nagaraj, B. V. T. Rao, S. N. Chintalapudi, and S. S. Ghugre, Pramana **54**, 347 (2000).
[17] D. C. Radford, Nucl. Instrum. Methods Phys. Res. A **361**, 297 (1995).
[18] M. Lach *et al.*, Z. Phys. A **345**, 427 (1993).
[19] M. A. Cardona, G. de Angelis, D. Bazzacco, M. De Poli, and S. Lunardi, Z. Phys. A **340**, 345 (1991).
[20] S. Juutinen *et al.*, Phys. Rev. C **51**, 1699 (1995).